Translational Oncology
www.transonc.com

Volume 11 Number 3 June 2018 pp. 743–754 743

The Role of Promyelocytic Leukemia Protein in Steatosis-Associated Hepatic Tumors Related to Chronic Hepatitis B virus Infection[1]

Yih-Lin Chung* **and Mei-Ling Wu†**

*Department of Radiation Oncology, Koo Foundation Sun-Yat-Sen Cancer Center, Taipei 112, Taiwan; †Department of Pathology and Laboratory Medicine, Koo Foundation Sun-Yat-Sen Cancer Center, Taipei 112, Taiwan

Abstract

The persistence of hepatitis B surface antigen (HBsAg) is a risk factor for the development of steatosis-associated tumors in chronic hepatitis B virus (HBV) infection, yet little is known about the metabolic link with this factor. We correlated HBV-related pathogenesis in genetically engineered mice and human carriers with metabolic proteomics and lipogenic gene expression profiles. The immunohistochemistry showed that the promyelocytic leukemia protein (PML, a tumor suppressor involved in genome maintenance and fatty acid oxidation), being inversely influenced by the dynamic HBsAg levels from acute phase to seroclearance, appeared as a lipo-metabolic switch linking HBsAg-induced steatosis (lipogenesis) to HBsAg-lost fat-burning hepatocarcinogenesis (lipolysis). Knockdown of *PML* in *HBsAg*-transgenic mice predisposed to obesity and drove early steatosis-specific liver tumorigenesis. Proteome analysis revealed that the signaling pathways corresponding to energy metabolism and its regulators were frequently altered by suppression or depletion of PML in the *HBsAg*-transgenic mice, mainly including oxidative phosphorylation and fatty acid metabolism. Expression profiling further identified upregulation of stearoyl-CoA desaturase 1 (Scd1) and epigenetic methylation of *NDUFA13* in the mitochondrial respiratory chain and the cell cycle inhibitor *CDKN1c* in concordance to the increased severity of lipodystrophy and neoplasia in the livers of *HBsAg*-transgenic mice with PML insufficiency. The defect in lipolysis in PML-deficient *HBsAg*-transgenic mice made the HBsAg-induced adipose-like liver tumors vulnerable to synthetic lethality from toxic saturated fat accumulation with a Scd1 inhibitor. Our findings provide mechanistic insights into the evolution of steatosis-associated hepatic tumors driven by reciprocal interactions of HBsAg and PML, and a potential utility of lipid metabolic reprogramming as a treatment target.

Translational Oncology (2018) 11, 743–754

Introduction

Carriers of hepatitis B virus (HBV) may die of liver cirrhosis and/or hepatocellular carcinoma (HCC) [1]. Although HBV, a partly double-stranded DNA virus, is not cytopathic, clinical outcomes seem to depend on the extent of liver damage resulting from the complex interplay between virus latency and host immune response [2]. However, some clinical studies also reported a positive association between obesity and type II diabetes with an increasing incidence of HCC [3]. HCC is now the leading cause of obesity- or metabolism-related cancer deaths [4]. Whether there is a molecular link between metabolic changes and hepatocarcinogenesis in chronic HBV carriers remains unclear.

The 3.2-kb HBV genome encodes viral proteins essential to its life cycle, including DNA polymerase; the capsid protein hepatitis B core antigen (HBc); the L, M, and S envelope or surface (HBsAg) proteins; and protein X (HBx) [5]. During chronic latent HBV infection, the levels or expression of HBV-derived RNAs, DNAs and proteins

Address all correspondence to: Yih-Lin Chung, Department of Radiation Oncology, Koo Foundation Sun Yat-Sen Cancer Center, No.125, Lih-Der Road, Pei-Tou district, Taipei 112, Taiwan.
E-mail: ylchung@kfsyscc.org
[1] Declarations of interest: none.
Received 30 December 2017; Revised 29 March 2018; Accepted 29 March 2018

1936-5233

become undetectable, with the exception of HBsAg, whose clearance rate is very slow at approximately 0.7% per year [6]. HBsAg accumulation in the endoplasmic reticulum (ER) induces cellular stress, unfolded protein responses (UPRs) and DNA damage [7]. Because ER stress can cause fatty liver disease, also known as hepatic steatosis, the long-term stimulation of HBsAg appears to reprogram metabolism in a characteristic pattern during hepatocarcinogenesis [8].

The control of the metabolic switch by oncogenes and tumor suppressor genes is a key step in tumorigenesis [9]. Our previous studies have shown that, in the presence of HBsAg alone, the tumor suppressor promyelocytic leukemia protein (PML) was significantly degraded by the proteasome-mediated pathway [10]. PML is also an unexpected driver of fatty acid oxidation [11–13], and loss of *PML* leads to body fat accumulation [14]. HBsAg-induced steatosis prompts us to ask whether the HBsAg-associated PML degradation causes HBV to become a "metabolovirus" and causes lipid metabolic reprogramming during HCC development.

The present study provides novel insights into a bioenergetic adaptation induced by a mutually exclusive reciprocal interaction between HBsAg and PML in chronic HBV-related pathogenesis. The results of the present study demonstrate that targeting fatty acid metabolism may provide a therapeutic benefit in a subset of steatosis-associated HCCs.

Materials and Methods

Mice

PML$^{-/-}$ mice (129/SV-*Pml*$^{tm/Ppp}$ from the National Cancer Institute, USA) were crossed with liver-specific *HBsAg*-transgenic mice (C57BL/6 J-Tg(Alb1HBV)44Bri/J from Jackson Lab, USA) [15,16]. The resulting offspring were then crossed to produce different mouse genotypes, including *wild-type, PML*$^{+/-}$, *PML*$^{-/-}$, *PML*$^{+/+}$*HBsAg*$^{tg/0}$, *PML*$^{+/-}$*HBsAg*$^{tg/0}$, and *PML*$^{-/-}$*HBsAg*$^{tg/0}$, after several generations. These strains had similar genetic backgrounds (129/SV x C57BL/6 J) and were confirmed by whole exome sequencing, PCR genotyping, and immunohistochemistry. For nutrition challenge, mice were randomly assigned to a high-fat (HF) diet (TD.06414; Harlan Teklad) or a control diet (TD.08806; Harlan Teklad), and food intake and activity were measured in metabolic chambers. All mice were cared for according to NIH-approved institutional animal care guidelines with approval from the Institutional Animal Care and Use Committee. The animal protocol was approved by the Institutional Review Board of the Koo Foundation Sun Yat-Sen Cancer Center, Taipei, Taiwan. The mice were housed and maintained at the National Laboratory Animal Center in Taiwan under institutionally approved conditions.

Histopathology and Immunohistochemistry

The immunohistochemical analysis of archival paraffin blocks from 5 normal and 155 HBV-infected patients was approved by the Institutional Review Board of the Koo Foundation Sun Yat-Sen Cancer Center, Taipei, Taiwan. The liver tissue arrays from the 155 HBV-infected patients were further stratified by their clinical phases of HBV infection. Tissues samples from mice were collected following the recommendations provided in the Declaration of Helsinki and its amendments.

Human and mouse tissues were formalin fixed, dehydrated, and embedded in paraffin. Deparaffinized sections (4–5 μm) were treated with 1% H_2O_2 to block endogenous peroxidase activity and immersed in boiling 0.01% citric acid (pH 6.0) in a microwave oven for 15 min to enhance antigen retrieval. After cooling, the sections were rehydrated with PBS and stained with hematoxylin and eosin (H&E) or treated with the following antibodies: anti-PML, anti-HBsAg, anti-Ki-67, and anti-Scd1 (all from Santa Cruz Biotechnology, Dallas, Texas, USA). Immunohistochemistry was performed using the ABC Kit (Dako).

Drug Treatment

The SCD1 inhibitor A939572 (Biofine) was dissolved in alkmulphor/EtOH/saline solution (1:1:18). Total volumes of 50 to 100 μL of solution with or without A939572 (5 mg/kg) were injected intraperitoneally every other day for 4 weeks. Symptoms and signs of toxicities, including hair loss, lethargy, and changes in skin pigmentation, physical activity, food consumption, and body weight, were evaluated once each week. One month after completing the 4-week drug treatment, mouse livers were examined grossly and then sectioned for pathology.

Proteomics and Gene ontology (GO) Enrichment Pathway Analysis

Freshly frozen washed liver tissues were minced using mechanical homogenization and vigorous mixing. Proteins were extracted into lysis buffer (0.1 M Tris (hydroxymethyl)-aminomethane, pH 7.6 (Sigma, St. Louis, MO, USA); 0.1 M dithiothreitol (Promega, Madison, WI); and 10 μL/mL of HaltTM EDTA-free protease and phosphatase inhibitor cocktail (Thermo Scientific, Waltham, MA, USA)) and solubilized by heating in the presence of sodium dodecyl sulfate (Sigma, St. Louis, MO, USA). The clarified lysate was desalted with lysis buffer, which was exchanged with a series of buffers while simultaneously undergoing digestion with mass spectrometry (MS)-grade trypsin (Pierce-Thermo Scientific, Rockford, IL, USA). The digested peptides were identified using an externally calibrated high-resolution electrospray tandem Thermo LTQ Orbitrap Velos nLC-ESI-LIT-Orbitrap mass spectrometer at room temperature with 10 data-dependent collisional-induced-dissociation MS/MS scans per full scan under the direct control of the Xcalibur software (Thermo Scientific, Waltham, MA, USA). The peptide threshold was 95% confidence, and the stringency for proteins was 99% confidence with at least 2 peptide matches.

Proteins with more than a 2-fold change in expression level in genetically engineered transgenic or knockout mice relative to those levels in matched wild-type mice were analyzed using the Database for Annotation, Visualization and Integrated Discovery (DAVID) Bioinformatics resource and Protein Analysis Through Evolution Relationships (PANTHER) classification system to identify enriched gene ontology (GO) terms [17–19]. The likelihood of overrepresentation of GO categories was calculated using Fisher's exact test. Enriched pathways associated with the differentially expressed proteins were also analyzed using GeneGO pathway maps in the MetaCore™ database (version 6.24; build 67,895, Thomson Reuters). The Mann–Whitney *U* test was used to assess the statistical significance of intergroup differences, and a p-value of less than 0.05 was considered significant.

Quantitative Real-time RT-PCR

Total RNA from the liver was extracted using Trizol (Invitrogen) and purified by DNA digestion using an RNeasy Kit (QIAGEN). cDNAs were synthesized using the GoScriptTM Reverse Transcription System (Promega, Fitchburg, WI). For qPCR, the primers for all genes and TaqMan probes were obtained from Applied Biosystems. A

7900 Real-Time PCR System and a VIIA7 Real-Time PCR System (Applied Biosystems) were used for qPCR. Expression levels were normalized to 18S rRNA levels. The relative mRNA levels were calculated using the $2^{-\Delta\Delta Ct}$ method.

Gene Methylation Analysis

Genomic DNA was extracted using the DNeasy Blood and Tissue Kit (QIAGEN). A PCR-based quantitative methylation analysis was performed using an EpiTect Methyl II PCR Array kit (QIAGEN) according to the manufacturer's instructions. Genomic DNA (1 μg) was incubated with or without specific methylation-dependent or methylation-sensitive restriction enzymes and subjected to real-time PCR with SYBR green. For methylation analysis, the primers for all genes were obtained from QIAGEN. The PCR protocol included an initial hot start at 95 °C for 10 min, followed by 3 cycles of 99 °C for 30 s and 72 °C for 1 min, and then 40 cycles of 97 °C for 15 s and 72 °C for 1 min. The gene methylation status was determined as the percentage of unmethylated and methylated fractions of input DNA by comparing the intensity of SYBR Green fluorescence detected during the annealing step of each cycle between samples with or without specific methylation-dependent or methylation-sensitive restriction enzymes.

Results

Association of PML with HBsAg-induced Steatosis in Mice

We first inspected the metabolic alterations in pathology and pathogenesis of the liver-specific *HBsAg*-transgenic ($HBsAg^{tg/0}$) mice. The hepatocytes with HBsAg accumulation exhibited ground glass change by 6 months of age (Figure 1*A*). This was followed by progressive loss of HBsAg, increased lipid storage (steatosis) by 10 months of age, and dysplasia at 14 months of age. The timing of development and the severity and prevalence of HBsAg-induced pathology with steatosis, dysplasia, adenoma and HCC in chronological order in $HBsAg^{tg/0}$ male mice were earlier and greater as opposed to females, which reiterated the natural course of HBV pathogenesis and male predominance in humans [20,21]. Moreover, the HBsAg-induced pathogenesis from early ground-glass change, steatosis to later dysplasia occurrence was correlated with a gradually reciprocal expression pattern between HBsAg and PML from $HBsAg^{high}/PML_{suppression}$ to $HBsAg^{lost}/PML_{restored}$. Unlike disruption in leukemia cells, we have previously shown that *PML* is not mutated in HBV-related HCC [20,22]. Because PML functions not only to maintain genome stability but also to enhance fatty acid oxidation [10–14,20,23], the reciprocal interaction between HBsAg and PML might link steatosis to tumorigenesis.

PML as a Metabolic Switch between Lipogenesis and Lipolysis

We then performed metabolic proteomic profiling of liver extracts from *wild-type*, $HBsAg^{tg/o}$, $PML^{-/-}$ and $PML^{-/-}HBsAg^{tg/0}$ mice with different ages. Consistent with the known biological effects of HBsAg on ER stress, UPRs and immunogenicity, proteomic analysis of the canonical GO pathway enrichment distribution in a set of 650 signaling and metabolic maps revealed that many differentially regulated proteins in $HBsAg^{tg/0}$ mice were involved in energy metabolism, protein processing and immune response (Figure 1*B*, Supplementary Figure S1 and Table S1). In line with the observed HBsAg-induced PML suppression in 6-month-old mice, the liver proteomics of $HBsAg^{tg/0}$ mice also demonstrated an altered feature highly overlapping with that of *PML*-knockdown ($PML^{-/-}$) mice when compared to that of the age- and sex-matched wild-type mice (Supplementary Figure S2). In $PML^{-/-}$ mice, pathway alterations also corresponded to the roles of PML in DNA damage response and cell cycle regulation. However, energy metabolism and its regulators, including increased oxidative phosphorylation, glucose and fatty acid metabolism and tricarboxylic acid cycle for ATP generation in particular, were the most active biological processes in all of the $PML^{-/-}$, $HBsAg^{tg/0}$ and $PML^{-/-}HBsAg^{tg/0}$ mice (Supplementary Figure S3 and Table S2). This result indicates that the presence of HBsAg and/or loss of PML primarily affected the metabolic factory of the cell and the mitochondria and induced an analogous metabolic reprogramming at the initial stage.

In order to provoke, evaluate and define the metabolic role of PML in condition of HBsAg presence, we used a HF diet to challenge *wild-type*, $PML^{-/-}$, $PML^{+/+}HBsAg^{tg/0}$, $PML^{+/-}HBsAg^{tg/0}$ and $PML^{-/-}HBsAg^{tg/0}$ mice; these mice displayed a spectrum of differential ratios of HBsAg/PML expression (Supplementary Figure S4, *A* and *B*). The distinct liver pathologies augmented by the HF diet challenge between *wild-type*, $PML^{-/-}$, $PML^{+/+}HBsAg^{tg/o}$, $PML^{+/-}HBsAg^{tg/0}$ and $PML^{-/-}HBsAg^{tg/0}$ mice at 8–10 months of age revealed time- and dosage-dependent effects of PML loss or insufficiency on the severity of lipogenesis (manifested by ballooned-type liver cells) and of HBsAg accumulation and the extent of ER stress (manifested by ground-glass change, mild steatosis and dysplasia). As expected, the synergistic or summed effects of PML loss and HBsAg accumulation augmented the lipid metabolic disorders in $PML^{-/-}HBsAg^{tg/0}$ mice (Supplementary Figure S4*C*). $PML^{-/-}HBsAg^{tg/0}$ mice had significantly accelerated rates of weight gain and body fat accumulation and increased liver weight compared to those in *wild-type*, $PML^{-/-}$, and $PML^{+/+}HBsAg^{tg/o}$ HF-fed mice by 6 months of age. In contrast, no differences were observed in HF diet consumption (mean 8.5–10.0 Kcal/day) between each group. The obesity phenotype with substantial increases in visceral and subcutaneous white-fat masses in $PML^{-/-}HBsAg^{tg/0}$ HF-fed mice became obvious by 10–12 months of age. Because both human and mouse pathology consistently demonstrated that lipogenesis occurred at the initial stage with $HBsAg^{high}/PML_{low}$ and that lipolysis occurred at the later stage with $HBsAg^{low}/PML_{high}$, the restoration of PML leading to the inverse conversion of the HBsAg/PML expression ratio (while HBsAg was lost with time) could be a critical turning point in lipid or energy metabolic reprogramming during HBV-related pathogenesis.

Loss of PML Drives Early Development of Steatosis-associated Hepatic Tumors

To demonstrate the metabolic consequences of long-term PML suppression in HBsAg-expressing liver cells, administration of the HF diet was extended to 11 months in $PML^{-/-}HBsAg^{tg/0}$ mice. Unexpectedly, although liver weight increased continuously, the size of the white-fat mass in obese mice decreased (Supplementary Figure S5*A*). Upon histological examination over time, we found that the white visceral and cutaneous fats started browning-like wasting in 9-month-old mice prior to the loss of the body white-fat masses, whereas hepatic steatosis became increasingly severe over time (Supplementary Figure S5*B*). The contrast in lipid metabolic rates between the liver and the body white-fat tissues of the $PML^{-/-}HBsAg^{tg/0}$ mice was reminiscent of human HCC-associated cachexia, implying a metabolic demand for increasing energy expenditure. Moreover, the divergent alterations in the liver proteomics between 3-month-old and 9-month-old

PML$^{-/-}$*HBsAg*$^{tg/0}$ mice occurred mainly in pathways regulating chromatin remodeling, apoptosis and survival, fatty acid metabolism, oxidative phosphorylation and cell cycle, which are all hallmarks of cancer (Supplementary Figure S5*C* and Table S3).

Consistently, numerous pale, enlarged white nodular tumors of various diameters were observed on the surfaces of livers from the previously obese *PML*$^{-/-}$*HBsAg*$^{tg/0}$ HF-fed male mice with hepatomegaly and body fat loss at 10 months of age (Figure 2). Further liver

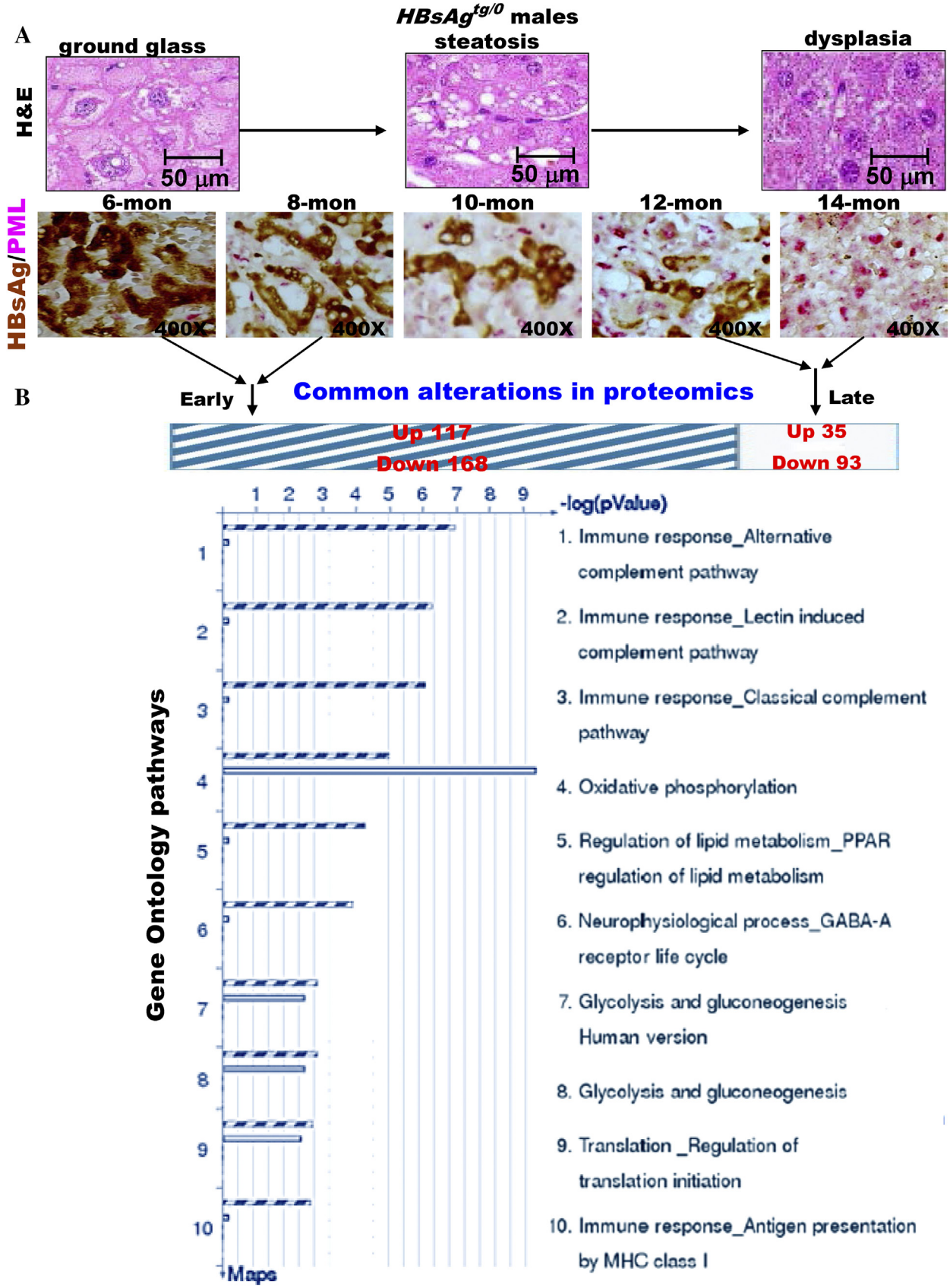

histological examination confirmed the development of multiple well-defined spot-like pale adenomas and early-onset invasive adipose-like HCCs arising from the adenomas. In contrast, in the presence of *PML*, both $PML^{+/-}HBsAg^{tg/0}$ and $PML^{+/+}HBsAg^{tg/0}$ HF-fed male mice were relatively lean and did not develop HCC until 14–24 months of age. The late-onset HCC in the $PML^{+/+}HBsAg^{tg/0}$ HF-fed male mice at 18 months of age appeared as a rapidly progressive large angiogenic tumor in a trabecular pattern without marked fat droplets, which indicated that the previous steatosis was burnt out. Interestingly, in $PML^{+/-}HBsAg^{tg/0}$ HF-fed male mice, the contrasting amount of lipid accumulation between HCC cells and the surrounding liver cells, the timing of HCC development at 14 months of age, and the varied mosaic angio-lipogenic HCC pathology appeared to be a mixed pathogenic feature of $PML^{-/-}HBsAg^{tg/0}$ and $PML^{+/+}HBsAg^{tg/0}$ mice, indicating haploinsufficiency of PML in lipid metabolism during HBsAg-induced hepatocarcinogenesis. Moreover, in the $PML^{+/-}HBsAg^{tg/0}$ mice, the sharp boundary between the severe fatty changes of the surrounding non-tumor portion of livers and the strikingly decreased fat content of HCCs corresponded to distinct expression patterns separating $PML^{suppressive}/HBsAg_{extensive}$ and $PML^{intensive}/HBsAg_{lost}$ areas, suggesting the prominence of pale appearance resulting from the amount of lipid accumulation observed in the tumors was inversely correlated the dosage of PML expression which was affected by the HBsAg expression. In summary, our results demonstrate that PML acts as a molecular switch involved in metabolic reprogramming between lipogenesis and lipolysis and is associated with HBsAg-induced HCC progression.

Synthetic Lethal Therapy for PML-deficient Steatosis-associated Hepatic Tumors

Next, we aimed to identify potential treatment targets of the PML-associated lipid metabolic reprogramming for HBsAg-induced HCC. Pathway-focused gene expression profiling by semi-quantitative RT-PCR was performed in *HBsAg*-transgenic mice with a spectrum of different ratios between liver PML and HBsAg expression and distinct pathological features (Figure 3*A*). We found that some of lipogenic genes, such as *sterol regulatory element-binding transcription factor 2* (*SREBF2*), *3-hydroxy-3-methyl-glutaryl-coenzyme A reductase* (*HMGCR*), *peroxisome proliferator-activated receptor gamma* (*PPAR-γ*) and *Scd1*, were elevated in HCCs (Figure 3*B*). However, only *Scd1* showed a differential expression between the normal livers and HCCs. *Scd1* has been reported to be under the control of the lipogenic transcriptional factor *SREBF1* [24]. Our result did not demonstrate concordant changes of *Scd1* and *SREB1* which, in contrast, appeared to be decreased in the HCCs, suggesting *Scd1* was up-regulated through other mechanisms in our model. As compared to *Scd1*, no correlative association was observed between normal livers, HCCs and the expression of principal genes involved in damage or immune responses (such as *TNF-α, IL-6, STAT3,* and *IL-1β*) and apoptosis and survival (such as *Fas, Bax and Bcl-2*) (Figure 3*C*). The clustered heat map further revealed *Fads1* and *Fads2* (encoding desaturases for polyunsaturated fatty acid synthesis) were coregulated with *Scd1* (forming monounsaturated fatty acids) along the course of hepatocarcinogenesis (Figure 4*A*), indicating the increased lipogenesis and the balance between saturated and unsaturated fatty acids could be predictors for HBsAg-induced HCC development. Consistently, gradual up-regulation of *Scd1* was also associated with epigenetically progressive down-regulation of *NDUFA13* (also known as *GRIM-19*; encoding a component of the mitochondrial electron-transfer complex I for oxidative phosphorylation) and *CDKN1c* (encoding a cell cycle inhibitor), which are hallmarks leading to hepatocarcinogenesis (Figure 4*B* and Supplementary Table S4). Moreover, not only the *Scd1* mRNA but also the Scd1 protein exhibited gradual up-regulation in correlation of pathological progression from normal liver, steatosis, dysplasial change to HCC development (Figure 4*C*).

Elevated Scd1 expression was observed during the initial lipogenic phase of HBsAg-induced pathogenesis leading to hepatocarcinogenesis in both $PML^{+/+}HBsAg^{tg/0}$ and $PML^{-/-}HBsAg^{tg/0}$ mice, but the accumulated lipid in the livers was consumed at different rates in the $PML^{+/+}HBsAg^{tg/0}$ and $PML^{-/-}HBsAg^{tg/0}$ mice after PML was restored in the $PML^{+/+}HBsAg^{tg/0}$ mice. Because Scd1 inhibition induces the accumulation of saturated fatty acids that are toxic to cells and PML suppression prevents lipolysis that could fuel tumor growth [11,23,25], the fat-accumulating HCC (lipogenesis phenotype) of $PML^{-/-}HBsAg^{tg/0}$ mice should be more vulnerable to the Scd1 inhibitor, and the angiogenic HCC (lipolysis phenotype) of $PML^{+/+}HBsAg^{tg/0}$ mice should be more sensitive to arsenic trioxide that degrades PML, which is a treatment strategy that leads to synthetic lethality. Our previous study showed that PML inhibition with a non-toxic dose of arsenic trioxide (As_2O_3) selectively killed long-term HBsAg-affected liver cells in PML-positive $HBsAg^{tg/o}$ mice with falling HBsAg levels and rising PML levels but not normal liver cells or early-onset HCC cells in PML-negative $HBsAg^{tg/0}$ mice [22]. Consistently, in parallel with the selectively therapeutic effect of As_2O_3 on $PML^{+/+}HBsAg^{tg/o}$ mice [22], the killing effect of pharmacologic Scd1 inhibition on inducing fatty cell necrosis in the present study only appeared on the adipose-like HCCs of $PML^{-/-}HBsAg^{tg/0}$ mice (Figure 5*A*) but not on the normal liver cells of *wild-type* mice, the normal-like liver cells of $PML^{-/-}$ mice, the dysplasial liver cells of $HBsAg^{tg/0}$ mice (Figure 5*B*), or the late-onset fatless angiogenic HCCs in $PML^{+/+}HBsAg^{tg/0}$ mice (Figure 5*C*).

PML Links Steatosis to Human HBV-related HCC

Thus, in order to see if the relationship of PML and HBsAg in the steatosis-associated pathogenesis observed in mice could be recapitulated in chronic human HBV-infected liver pathology, we then examined tissue arrays by immunostaining with anti-HBsAg and anti-

Figure 1. Reciprocal interactions of PML and HBsAg is closely associated with metabolic reprogramming in a chronic HBV mouse model. (A) Representative double-stained images of PML and HBsAg in liver-specific *HBsAg*-transgenic mice ($HBsAg^{tg/0}$) at different ages. Note that correlation of the evolving pathology in mice with reciprocal interactions between PML and HBsAg recapitulates the chronic human HBV-infected liver pathogenesis observed in Figure 1C. (B) Comparison of proteomic profiling between young and aged $HBsAg^{tg/0}$ mice. The enriched genes, whose expression was 2-fold up-regulated or down-regulated in more than 50% of the genetically engineered mice (n = 10 for each genotype) compared to the average expression of the same genes in sex- and age-matched *wild-type* mice (n = 5 for each group), were categorized by gene ontology (GO) analysis. Note that the major GO pathways affected in young mice with HBsAg-dominant expression and older mice with PML-dominant expression are involved in immune response and energy metabolism, respectively.

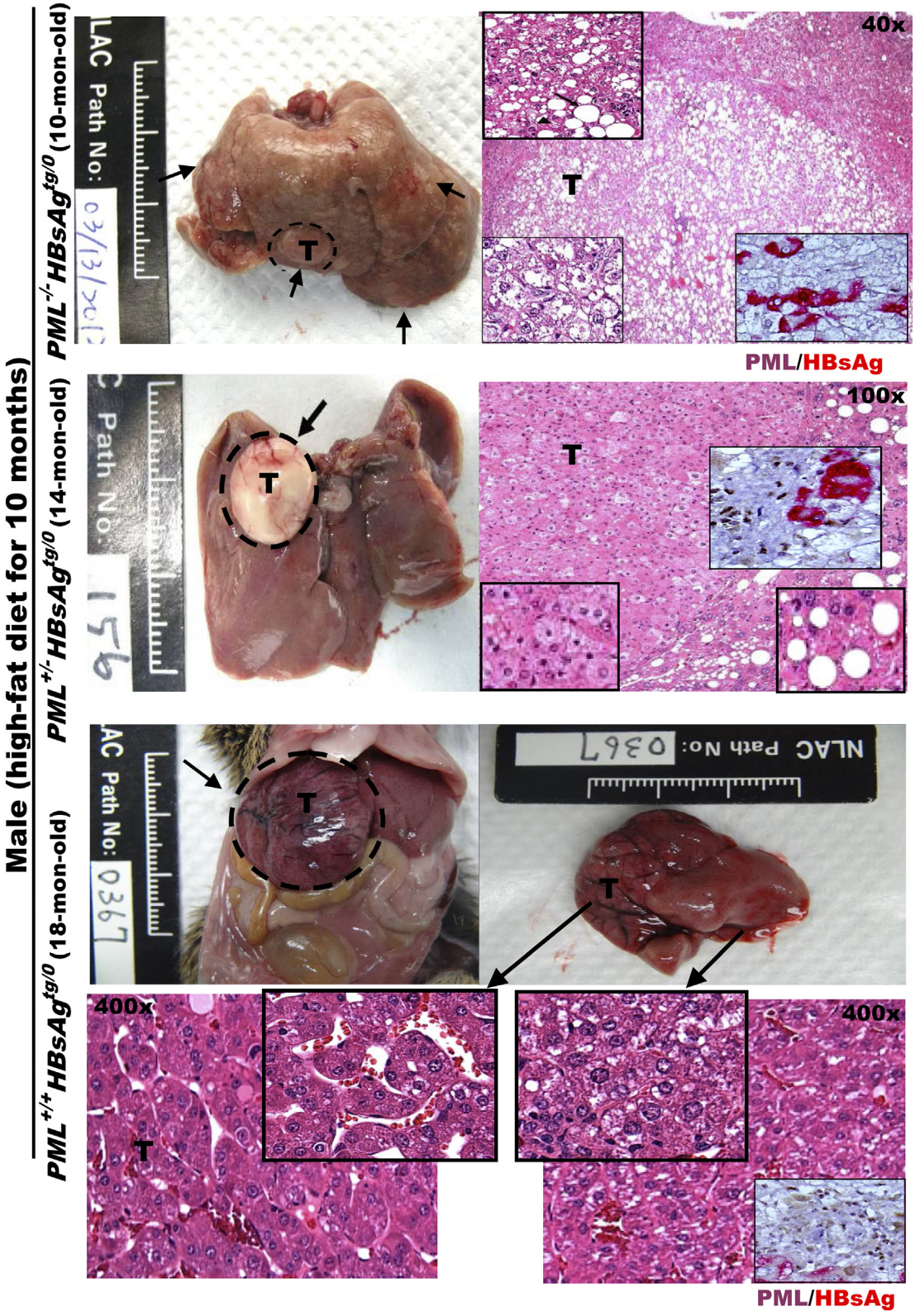

Figure 2. Altered PML expression levels reciprocally interacting with HBsAg levels correlate with distinct pathology and phenotypes of lipid metabolism and HBsAg-induced HCCs in mice. Representative images of gross livers and H&E histology with higher magnification of double immunostaining for PML (brown color in the nuclei) and HBsAg (red color in the cytoplasm) from *HBsAg*$^{tg/0}$ mice with or without one or two copies of *PML* knockdown are compared after HCC development. Note that *PML*$^{-/-}$*HBsAg*$^{tg/0}$, *PML*$^{+/+}$*HBsAg*$^{tg/0}$ and *PML*$^{+/-}$*HBsAg*$^{tg/0}$ mice display early-onset adipose-like solid-form HCC, late-onset fatless angiogenic trabecular-type HCC, and mixed adipose-angiogenic features of HCC, respectively. Squares represent in-situ zoomed regions.

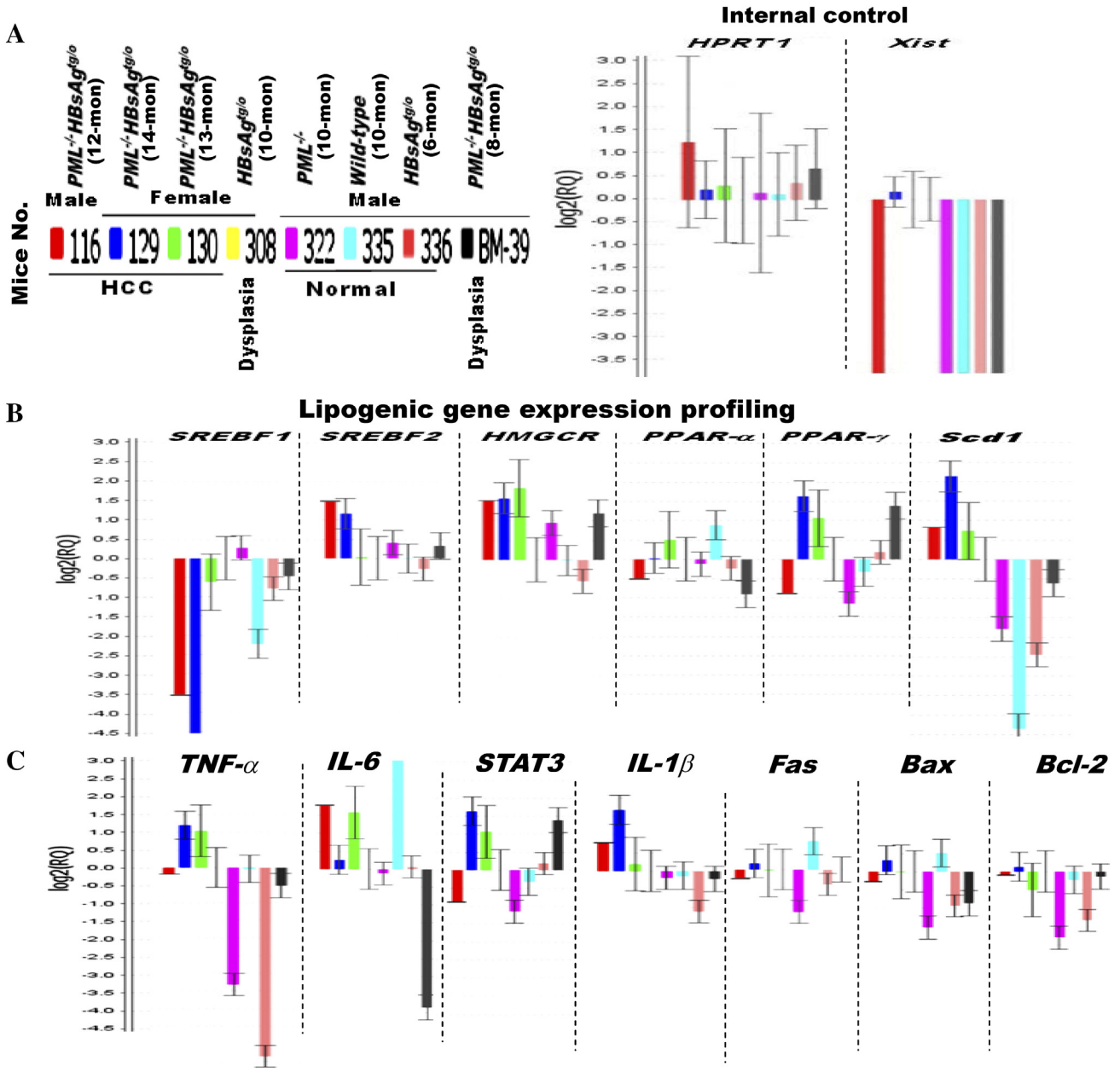

Figure 3. Different gene expression profiles of *HBsAg*-transgenic mice in the presence or absence of PML during HCC development. Comparison of **t**ranscriptional profiling in the livers of *wild-type*, *HBsAg*$^{tg/0}$, *PML*$^{-/-}$ and *PML*$^{-/-}$*HBsAg*$^{tg/0}$ mice with different ages, sex and pathology. (A) Internal control. (B) Lipogenic genes. (C) Inflammation and apoptosis genes. Error bars indicate mean ± SEM from 3 independent experiments. Note that the up-regulation of *Scd1* mRNA levels is in concordance with HCC development in *PML*$^{-/-}$*HBsAg*$^{tg/0}$ mice.

PML in a cohort of human liver biopsies from 160 patients with or without acute and chronic HBV infection (Figure 6, *A–B*). In parallel to the mouse model, the double-staining immunohistochemistry revealed a reciprocally negative interaction and mutually exclusive dynamic expression pattern between HBsAg and PML in the transition from acute hepatitis, chronic latent infection, steatohepatitis, and cryptogenic HCC development to invasive HCC progression (Figure 6*C*). Consistently, the expression of PML protein was suppressed in the HBsAg-expressing liver cells at the early phase of chronic infection. While in the late phase, progressive loss of the cytoplasmic HBsAg staining was synchronous with restoration of the nuclear PML staining, resulting in a sharp demarcation became notable between the fatless liver parts showing PML^{high}/HBsAg$_{lost}$ and the fatty liver areas showing PML^{lost}/HBsAg$_{high}$. Following re-appearance of PML in the HBsAg-lost liver cells during the course of cryptogenic HCC development, the fatty liver and fat droplets in the liver cells further disappeared, and exhibited a phenomenon of burnt-out steatosis in the PML-expressing liver cells. The results clearly demonstrated that PML expression inversely correlated with the severity and extent of HBsAg-induced steatosis in human HBV-infected liver cells.

Moreover, compared to the interior tumor cells with some spotted enhanced HBsAg staining (Figure 6*D*), the invasive front of advanced HCC with weak remnant or negative HBsAg staining

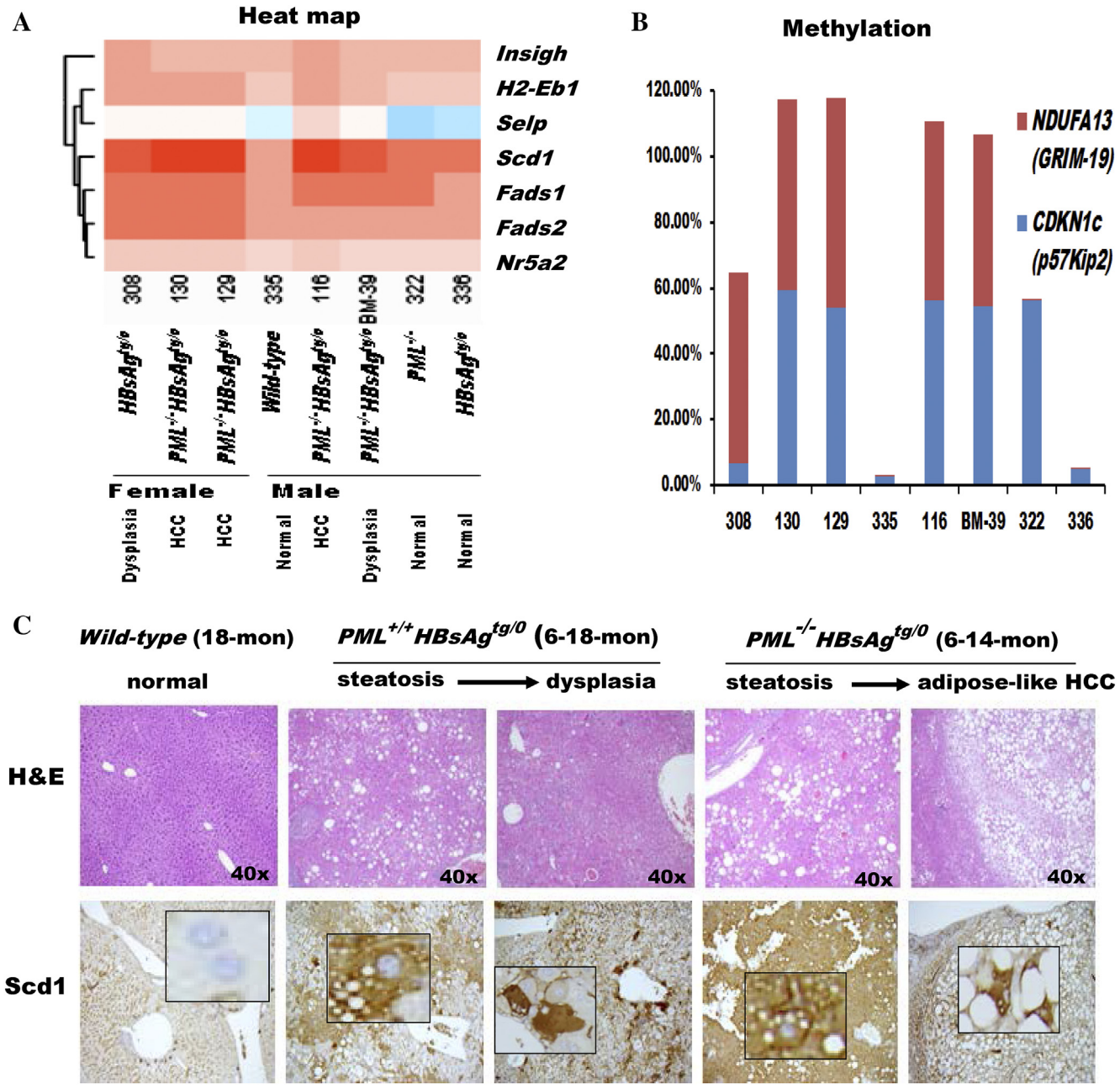

Figure 4. Correlation of liver pathology with gene expression toward hepatocarcinogenesis in the livers of *wild-type*, $HBsAg^{tg/0}$, $PML^{-/-}$ and $PML^{-/-}HBsAg^{tg/0}$ mice with different ages, sex and pathology. (A) Heat map demonstrating the cluster of differentially expressed genes related to lipid metabolism. Note that *Scd1*, *Fads1* and *Fads2* are desaturases involved in fatty acid synthesis and that Nr5a2 regulates cholesterol transport, bile acid homeostasis and steroidogenesis. (B) Epigenetic methylation analysis represented by percentage of growth control genes in livers from the same mice in (A). Note that, in addition to enhanced adipogenesis, *PML* loss is associated with impairment of the cell cycle and mitochondrial function during HBsAg-induced hepatocarcinogenesis. *NDUFA13* (also called *GRIM-19*), a subunit of the mitochondrial NADH dehydrogenase, functions in the transfer of electrons from NADH to the respiratory chain and as a tumor suppressor by binding to STAT3. *CDKN1c* (also called *p57Kip2*) encodes a strong inhibitor of G1 cyclin/Cdk complexes and a negative regulator of cell proliferation. (C) Correlation of liver histology with immunohistochemistry of Scd1 protein expression in *HBsAg*-transgenic mice with or without *PML* loss. Note that *PML* loss induces severe steatosis with diffusely enhanced Scd1 expression and early-onset adipose-like HCC in *HBsAg*-transgenic mice. Squares represent in-situ zoomed regions.

showed further up-regulation of PML along with increased Scd1. The concomitantly high expression of PML (involved in lipolysis), Scd1 (involved in lipogenesis) and Ki-67 (a cell proliferation index) signified active lipid metabolism in rapidly dividing human HBV-related HCC cells.

Discussion

Accumulation of HBsAg in the ER induces stress, which activates UPRs for protein degradation, and increases the lipid content of hepatocytes through unidentified mechanisms [8,26]. Surprisingly, the pronounced hepatic lipid accumulation disappeared over time in some HBV carriers

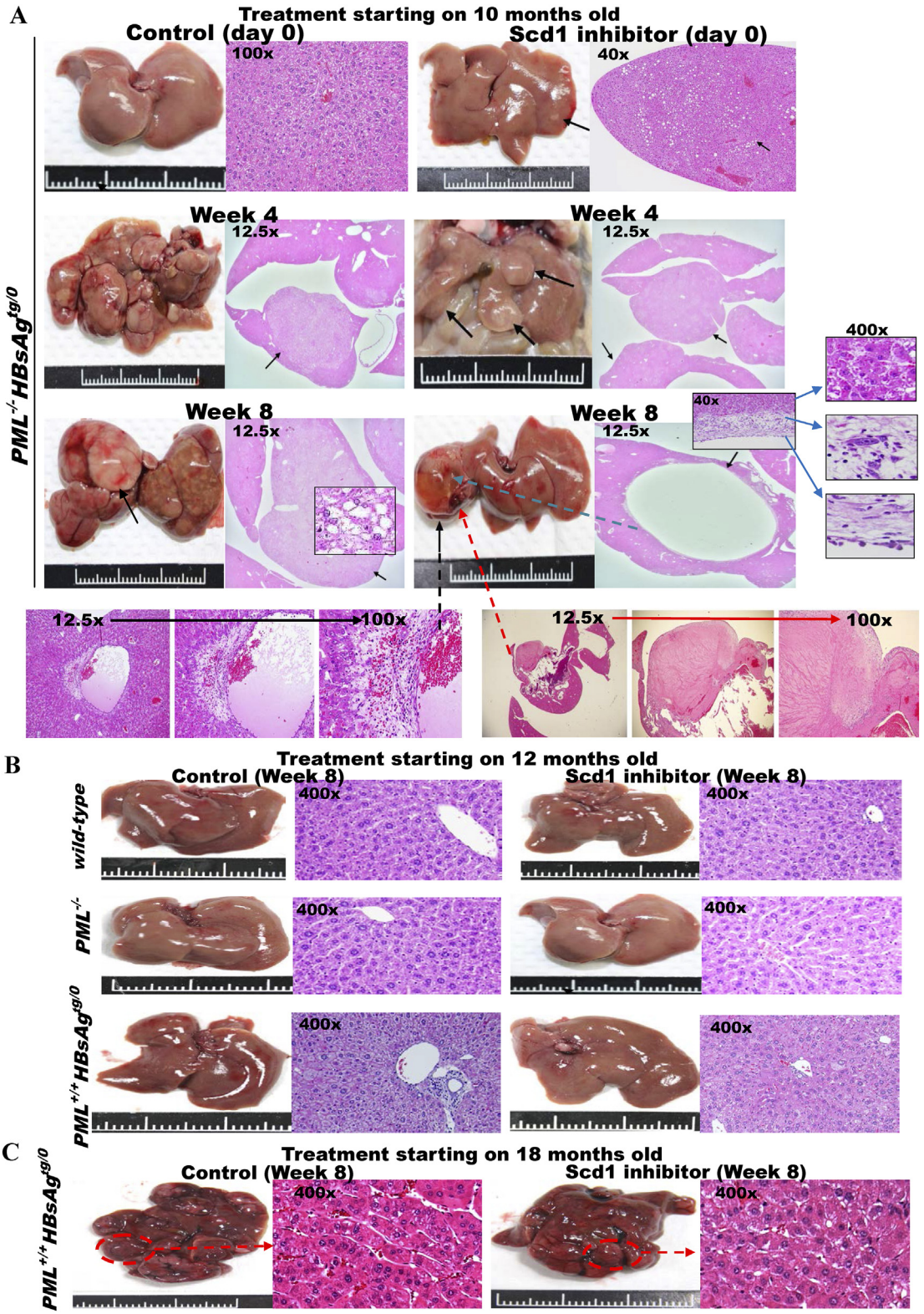

Figure 5. Scd1 is a metabolic therapeutic target for synthetic lethality in steatosis-associated hepatic tumors of *HBsAg*-transgenic mice with PML deficiency. Treatment with a small molecule Scd1 inhibitor, A939572, or solution control for *HBsAg*-transgenic mice with or without *PML* loss (n = 10–20 for each group). Representative images of gross livers and H&E histology are shown. (A) Ten-month-old $PML^{-/-}HBsAg^{tg/0}$ mice. Treatment was started when multiple early-onset adipose-like solid-form HCCs (arrows) were developing. Note that the Scd1 inhibitor regressed the HCCs by inducing necrosis of the fatty tumors and caused sinus ectasia with hemorrhage and cyst formation after resolution. (B) Twelve-month-old *wild-type*, $PML^{-/-}$ *and* $PML^{+/+}HBsAg^{tg/0}$ mice. Note that the treatment induced no cytotoxicity in normal liver cells or dysplasia. (C) Eighteen-month-old $PML^{+/+}HBsAg^{tg/0}$ mice. Note that the late-onset fatless or fat burnt-out angiogenic trabecular-type HCCs (broken circles) did not respond to the Scd1 inhibitor.

who developed cryptogenic HCC, a phenomenon of the so-called "burn-out steatosis" [27–30]. The molecular mechanism explaining the metabolic paradox in shifting from lipogenesis to lipolysis during HBV-related pathogenesis remains poorly understood.

In the present study, we demonstrated that dynamic HBsAg levels in the long-term course of HBV-related pathogenesis were completely, synchronously, and inversely correlated with corresponding fluctuations in PML expression in both human pathology and

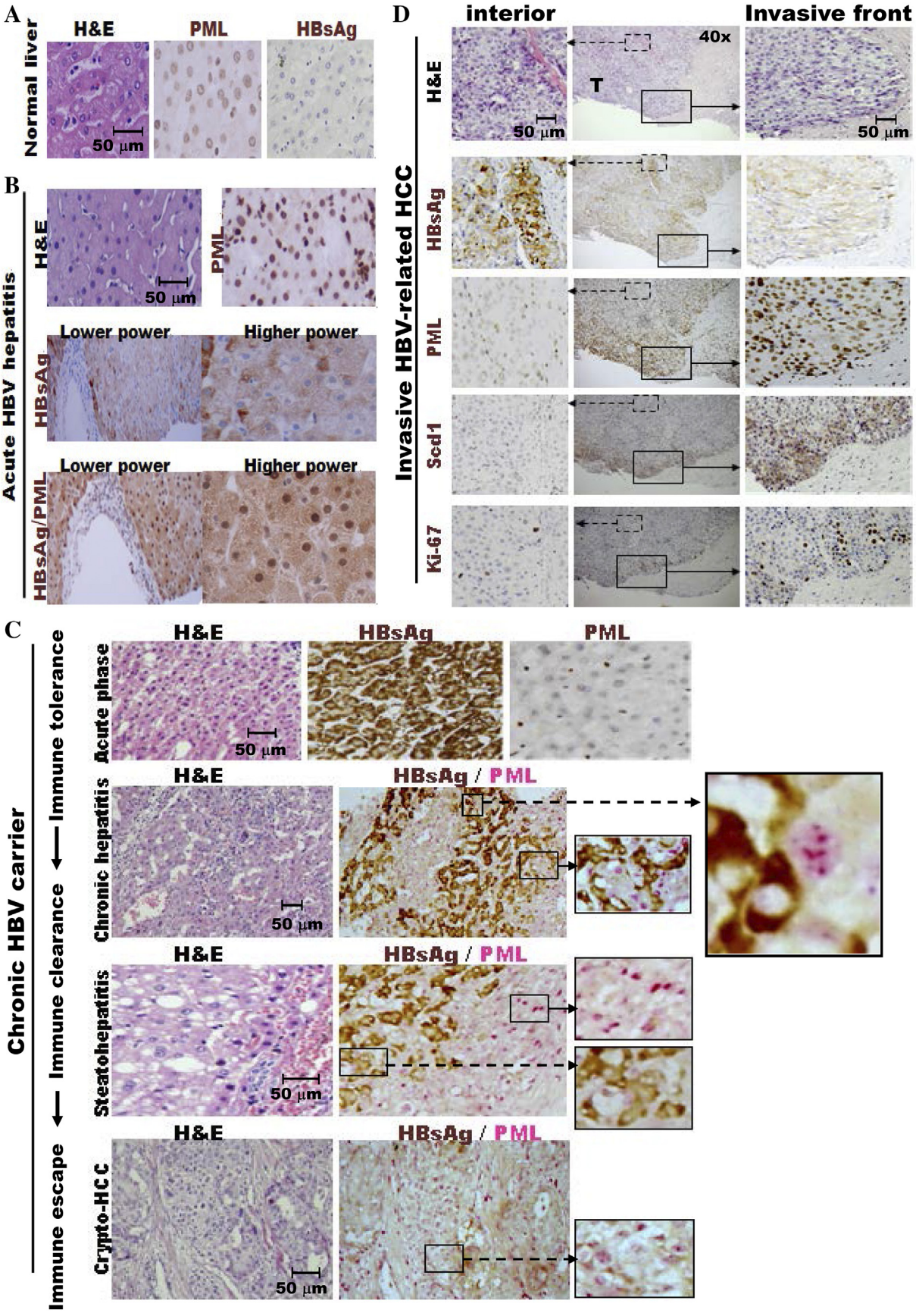

mouse models. Liver-specific *HBsAg*-transgenic mice displayed a spectrum of expression ratios from early $HBsAg^{high}/PML_{low}$ to later $HBsAg^{low}/PML_{high}$, which corresponded to a variety of phenotypes from lipogenesis to lipolysis, respectively. PML is relevant for responses to DNA damage, latent viral infections, oncogenic insults, metabolic challenges, nutritional disorders, obesity, and hepatic steatosis [10–15,20–23,31–35]. Thus, in view of the positive roles of PML in both suppression of tumor growth and activation of fatty acid oxidation pathways, our results imply that at the earlier phase of chronic HBV infection, HBsAg-induced ER stress and UPRs may degrade PML, leading to steatosis, obesity and tumor formation; in contrast, at the later HBsAg seroclearance phase, PML restoration can result in lipolysis, exhibiting burn-out steatosis.

Although our findings suggest that HBV could act as an "oncogenic metabolovirus" by targeting PML via HBsAg, PML suppression might not be the only factor responsible for HBV-induced fatty liver disease and hepatocarcinogenesis. HBsAg also targets the Na/taurocholate cotransporting polypeptide (SLC10A1), the HBV entry receptor overlapping with the transporter for bile acid at the plasma membrane of hepatocytes, to inhibit bile acid uptake and thus promote compensatory cholesterol provision [36]. Nevertheless, in our study, the severity of HBsAg-induced steatosis did not correspond to the expression of the rate-controlling enzyme *HMGCR* for cholesterol synthesis or the main lipogenic transcription factors *SREBF1* and *PPAR*. Instead, an increased expression of in Scd1, a desaturase that turns saturated lipids into unsaturated ones, was well correlated with steatosis and hepatocarcinogenesis in $HBsAg^{tg/0}$ mice with PML loss. In agreement with our study, previous studies also demonstrated that Scd1 overexpression was associated with predisposition to hepatocarcinogenesis [37]. However, genetic ablation of *Scd1* neither inhibited hepatic steatosis nor affected HCC development [38]. Because our proteomics and gene expression profile indicated impaired citric acid cycle and electron transport chain during HBsAg-induced hepatocarcinogenesis, up-regulation of Scd1 in correlation with the severity of fatty liver and adipose-like HCC development augmented by HF diet in $PML^{-/-}HBsAg^{tg/0}$ mice could result from the stimulation of saturated lipids extracted from the serum (due to HF diet), decreased fatty acid oxidation (due to PML deficiency), and de novo lipogenesis (due to defective mitochondrial function) [39]. Moreover, we also found that, while increasing hepatic fat content continuously, the *PML* knock-out mice with liver-specific *HBsAg*-transgene initially exhibited white body fat mass accumulation but showed rapid body fat browning and body mass wasting during later HCC progression. Therefore, some systemic factors connecting the liver and body adipose tissue might exist and contribute to the dysmetabolic cachexia state [28,40,41].

Recognition of HBsAg-induced HCCs as a spectrum or family of distinct metabolic diseases influenced by the reciprocal interaction of PML and HBsAg expression has implications for drug choice optimization. Regardless of PML suppression or degradation either as a direct target of HBsAg or as an indirect consequence of HBsAg-induced ER stress and due to the biological functions of PML in tumor growth regulation and fatty acid oxidation, presence of PML links "burn-out" steatosis (lipolysis) to late-onset HBsAg-induced angiogenic HCC progression, and loss of PML links steatosis and obesity (lipogenesis) to early-onset HBsAg-induced adipose-like HCC development. Thus, PML could be a metabolic biomarker for HBV-related HCC treatment. As shown in our previous study [22], for the fat-burning HCCs of $PML^{+/+}HBsAg^{tg/0}$ mice in which PML fueled fat for tumor progression, arsenic trioxide targeting PML for proteasome degradation was effective on slowing tumor progression. In comparison, as shown in the present study, for the steatosis-associated adipose-like HCCs of $PML^{-/-}HBsAg^{tg/0}$ mice in which PML acted as a tumor suppressor for genome maintenance and in which its loss led to early HCC predisposition and fat accumulation, synthetic lethality was achieved with the Scd1 inhibitor that induced toxic saturated fat accumulation. Therefore, determining how to overcome treatment resistance using a combination of arsenic trioxide for $PML^{high}/HBsAg_{low}$ and the Scd1 inhibitor for $PML^{low}/HBsAg_{high}$ through synthetic lethality on both metabolism and tumorigenesis warrants further investigation.

Conclusions

The present study demonstrates that the PML deficiency-mediated lipo-metabolic reprogramming induced by HBsAg appears to be a hallmark of chronic HBV-associated pathogenesis leading to steatosis-associated hepatocarcinogenesis.

Supplementary data to this article can be found online at https://doi.org/10.1016/j.tranon.2018.03.013.

Acknowledgements

This work was supported by grants from the Ministry of Science and Technology, Taiwan (MOST 104-2320-B-368-001) to Y. C.

References

[1] Raffetti E, Fattovich G, and Donato F (2016). Incidence of hepatocellular carcinoma in untreated subjects with chronic hepatitis B: a systematic review and meta-analysis. *Liver Int* **36**, 1239–1251.

[2] Guerrieri F, Belloni L, Pediconi N, and Levrero M (2013). Molecular mechanisms of HBV-associated hepatocarcinogenesis. *Semin Liver Dis* **33**, 147–156.

[3] Noureddin M and Rinella ME (2015). Nonalcoholic Fatty liver disease, diabetes, obesity, and hepatocellular carcinoma. *Clin Liver Dis* **19**, 361–379.

[4] Karagozian R, Derdák Z, and Baffy G (2014). Obesity-associated mechanisms of hepatocarcinogenesis. *Metabolism* **63**, 607–617.

[5] Dandri M and Petersen J (2016). Mechanism of Hepatitis B Virus Persistence in Hepatocytes and Its Carcinogenic Potential. *Clin Infect Dis* **62**(Suppl. 4), S281–8.

Figure 6. PML expression is inversely correlated with dynamic HBsAg levels in human chronic HBV-related pathogenesis. Representative H&E staining and immunostaining of PML (a regulator involved in DNA damage response and repair, cell death and survival, and fatty acid oxidation), HBsAg (an HBV component), Ki-67 (a cell proliferation marker) and/or Scd1 (a key enzyme in fatty acid synthesis) from a normal liver (A), acute HBV infection (B), a chronic HBV carrier (C), and an invasive HBV-related HCC (D). Clinically, chronic HBV pathogenesis can be subdivided into several phases: immune tolerance (high HBsAg levels), immune clearance (decreased HBsAg expression), immune escape (low HBsAg levels), and HCC formation (HBsAg loss). Note that nuclear PML immunoreactivity is strong in acute infection but suppressed in the early phase of chronic infection, which shows intensive cytoplasmic HBsAg staining. PML suppression is relieved upon clearance of HBsAg, indicating a reciprocal interaction between PML and HBsAg. PML restoration appears to correlate with gradually burnt-out steatosis during HCC development while HBsAg is lost. The simultaneously rising PML, Scd1 and Ki-67 immunoactivity in the invasive front of HBsAg-losing HCC cells reflects active fatty acid catabolism and anabolism coupled with cell proliferation. Zoomed regions indicated by arrows are shown in squares.

[6] Ferreira SC, Chachá SG, Souza FF, Teixeira AC, Santana RC, Villanova MG, Zucoloto S, Ramalho LN, Perdoná GS, and Passos AD, et al (2014). Factors associated with spontaneous HBsAg clearance in chronic hepatitis B patients followed at a university hospital. *Ann Hepatol* **13**, 762–770.

[7] Sunami Y, Ringelhan M, Kokai E, Lu M, O'Connor T, Lorentzen A, Weber A, Rodewald AK, Müllhaupt B, and Terracciano L, et al (2016). Canonical NF-κB signaling in hepatocytes acts as a tumor-suppressor in hepatitis B virus surface antigen-driven hepatocellular carcinoma by controlling the unfolded protein response. *Hepatology* **63**, 1592–1607.

[8] Baiceanu A, Mesdom P, Lagouge M, and Foufelle F (2016). Endoplasmic reticulum proteostasis in hepatic steatosis. *Nat Rev Endocrinol* **12**, 710–722.

[9] Levine AJ and Puzio-Kuter AM (2010). The control of the metabolic switch in cancers by oncogenes and tumor suppressor genes. *Science* **330**, 1340–1344.

[10] Chung YL (2013). Defective DNA damage response and repair in liver cells expressing hepatitis B virus surface antigen. *FASEB J* **27**, 2316–2327.

[11] Carracedo A, Weiss D, Leliaert AK, Bhasin M, de Boer VC, Laurent G, Adams AC, Sundvall M, Song SJ, and Ito K, et al (2012). A metabolic prosurvival role for PML in breast cancer. *J Clin Invest* **122**, 3088–3100.

[12] Ito K, Carracedo A, Weiss D, Arai F, Ala U, Avigan DE, Schafer ZT, Evans RM, Suda T, and Lee CH, et al (2012). A PML–PPAR-δ pathway for fatty acid oxidation regulates hematopoietic stem cell maintenance. *Nat Med* **18**, 1350–1358.

[13] Lallemand-Breitenbach V and de Thé H (2012). Hematopoietic stem cells burn fat to prevent exhaustion. *Cell Stem Cell* **11**, 447–449.

[14] Kim MK, Yang S, Lee KH, Um JH, Liu M, Kang H, Park SJ, and Chung JH (2011). Promyelocytic leukemia inhibits adipogenesis, and loss of promyelocytic leukemia results in fat accumulation in mice. *Am J Physiol Endocrinol Metab* **301**, E1130-2.

[15] Wang ZG, Delva L, Gaboli M, Rivi R, Giorgio M, Cordon-Cardo C, Grosveld F, and Pandolfi PP (1998). Role of PML in cell growth and the retinoic acid pathway. *Science* **279**, 1547–1551.

[16] Chisari FV, Klopchin K, Moriyama T, Pasquinelli C, Dunsford HA, Sell S, Pinkert CA, Brinster RL, and Palmiter RD (1989). Molecular pathogenesis of hepatocellular carcinoma in hepatitis B virus transgenic mice. *Cell* **59**, 1145–1156.

[17] Thomas PD, Kejariwal A, Campbell MJ, Mi H, Diemer K, Guo N, Ladunga I, Ulitsky-Lazareva B, Muruganujan A, and Rabkin S, et al (2003). PANTHER: a browsable database of gene products organized by biological function, using curated protein family and subfamily classification. *Nucleic Acids Res* **31**, 334–341.

[18] Huang DW, Sherman BT, and Lempicki RA (2008). Systematic and integrative analysis of large gene lists using DAVID bioinformatics resources. *Nat Protoc* **4**, 44–57.

[19] Huang DW, Sherman BT, and Lempicki RA (2009). Bioinformatics enrichment tools: paths toward the comprehensive functional analysis of large gene lists. *Nucleic Acids Res* **37**, 1–13.

[20] Chung YL and Wu ML (2013). Promyelocytic leukaemia protein links DNA damage response and repair to hepatitis B virus-related hepatocarcinogenesis. *J Pathol* **230**, 377–387.

[21] Giannitrapani L, Soresi M, La Spada E, Cervello M, D'Alessandro N, and Montalto G (2006). Sex hormones and risk of liver tumor. *Ann N Y Acad Sci* **1089**, 228–236.

[22] Chung YL and Wu ML (2016). Dual oncogenic and tumor suppressor roles of the promyelocytic leukemia gene in hepatocarcinogenesis associated with hepatitis B virus surface antigen. *Oncotarget* **7**, 28393–28407.

[23] Chung YL and Tsai TY (2009). Promyelocytic leukemia nuclear bodies link the DNA damage repair pathway with hepatitis B virus replication: implications for hepatitis B virus exacerbation during chemotherapy and radiotherapy. *Mol Cancer Res* **7**, 1672–1685.

[24] Postic C and Girard J (2008). The role of the lipogenic pathway in the development of hepatic steatosis. *Diabetes Metab* **34**, 643–648.

[25] von Roemeling CA, Marlow LA, Wei JJ, Cooper SJ, Caulfield TR, Wu K, Tan WW, Tun HW, and Copland JA (2013). Stearoyl-CoA desaturase 1 is a novel molecular therapeutic target for clear cell renal cell carcinoma. *Clin Cancer Res* **19**, 2368–2380.

[26] Zhou H and Liu R (2014). ER stress and hepatic lipid metabolism. *Front Genet* **5**, 112.

[27] Yoshioka Y, Hashimoto E, Yatsuji S, Kaneda H, Taniai M, Tokushige K, and Shiratori K (2004). Nonalcoholic steatohepatitis: cirrhosis, hepatocellular carcinoma, and burnt-out NASH. *J Gastroenterol* **39**, 1215–1218.

[28] van der Poorten D, Samer CF, Ramezani-Moghadam M, Coulter S, Kacevska M, Schrijnders D, Wu LE, McLeod D, Bugianesi E, and Komuta M, et al (2013). Hepatic fat loss in advanced nonalcoholic steatohepatitis: are alterations in serum adiponectin the cause? *Hepatology* **57**, 2180–2188.

[29] Claudel T and Trauner M (2013). Adiponectin, bile acids, and burnt-out nonalcoholic steatohepatitis: new light on an old paradox. *Hepatology* **57**, 2106–2109.

[30] Lee SS, Jeong SH, Byoun YS, Chung SM, Seong MH, Sohn HR, Min BY, Jang ES, Kim JW, and Park GJ, et al (2013). Clinical features and outcome of cryptogenic hepatocellular carcinoma compared to those of viral and alcoholic hepatocellular carcinoma. *BMC Cancer* **13**, 335–344.

[31] Cheng X, Guo S, Liu Y, Chu H, Hakimi P, Berger NA, Hanson RW, and Kao HY (2013). Ablation of promyelocytic leukemia protein (PML) re-patterns energy balance and protects mice from obesity induced by a Western diet. *J Biol Chem* **288**, 29746–29759.

[32] Wang S, Long J, and Zheng CF (2012). The potential link between PML NBs and ICP0 in regulating lytic and latent infection of HSV-1. *Protein Cell* **3**, 372–382.

[33] Rabellino A and Scaglioni PP (2013). PML Degradation: Multiple Ways to Eliminate PML. *Front Oncol* **3**, 60.

[34] Regad T and Chelbi-Alix MK (2001). Role and fate of PML nuclear bodies in response to interferon and viral infections. *Oncogene* **20**, 7274–7286.

[35] Carracedo A, Rousseau D, Douris N, Fernández-Ruiz S, Martín-Martín N, Weiss D, Webster K, Adams AC, Vazquez-Chantada M, and Martinez-Chantar ML, et al (2015). The promyelocytic leukemia protein is upregulated in conditions of obesity and liver steatosis. *Int J Biol Sci* **11**, 629–632.

[36] Geier A (2014). Hepatitis B virus: the "metabolovirus" highjacks cholesterol and bile acid metabolism. *Hepatology* **60**, 1458–1460.

[37] Falvella FS, Pascale RM, Gariboldi M, Manenti G, De Miglio MR, Simile MM, Dragani TA, and Feo F (2002). Stearoyl-CoA desaturase 1 (Scd1) gene overexpression is associated with genetic predisposition to hepatocarcinogenesis in mice and rats. *Carcinogenesis* **23**, 1933–1936.

[38] Li L, Wang C, Calvisi DF, Evert M, Pilo MG, Jiang L, Yuneva M, and Chen X (2013). SCD1 Expression is dispensable for hepatocarcinogenesis induced by AKT and Ras oncogenes in mice. *PLoS One* **8**e75104.

[39] Mullen AR, Wheaton WW, Jin ES, Chen PH, Sullivan LB, Cheng T, Yang Y, Linehan WM, Chandel NS, and DeBerardinis RJ (2011). Reductive carboxylation supports growth in tumour cells with defective mitochondria. *Nature* **481**, 385–388.

[40] Handa P, Maliken BD, Nelson JE, Morgan-Stevenson V, Messner DJ, Dhillon BK, Klintworth HM, Beauchamp M, Yeh MM, and Elfers CT, et al (2014). Reduced adiponectin signaling due to weight gain results in nonalcoholic steatohepatitis through impaired mitochondrial biogenesis. *Hepatology* **60**, 133–145.

[41] Dasarathy S (2014). Is the adiponectin-AMPK-mitochondrial axis involved in progression of nonalcoholic fatty liver disease? *Hepatology* **60**, 22–25.